

# GIS and Fuzzy Logic Modeling for Assessing Landslide Susceptibility in Kenya

Hafid Nanis<sup>1</sup>, Mohamed Aly<sup>2</sup>

<sup>1</sup>Department of Geosciences, University of Arkansas, Fayetteville, Arkansas USA & College of Engineering Technology, Zuwara Libya

<sup>2</sup>Associate Professor, Department of Geosciences, University of Arkansas, Fayetteville, Arkansas USA

\*\*\*

**Abstract** - *Landslide susceptibility modeling plays a crucial role in sustainable development and hazard mitigation strategies. Despite the presence of numerous landslide-prone areas in Kenya, previous research has failed to address them adequately. This study aims to fill this research gap by developing a comprehensive methodology for assessing landslide susceptibility in Kenya, employing a weighted Geographic Information System (GIS) and a fuzzy logic model. The major causative factors influencing landslides, including lithology, slope, elevation, soil type, land-cover, precipitation, distance to fault lines, distance to major drainages, distance to roads, and distance to earthquake-occurrence locations, were carefully investigated and weighted using the Analytical Hierarchy Process (AHP). The findings reveal that approximately 26% of Kenya's total area is susceptible to landslides. Through the integration of the weighted overlay and fuzzy logic models, four distinct landslide-vulnerability zones were identified: low, medium, high, and very high. To validate the models, a dataset of 130 historical landslides was employed. Remarkably, the highest zone of landslide vulnerability identified by the weighted overlay and fuzzy logic models coincided with about 97% and 85% of the past landslide events, respectively. These results attest to the reliability of the developed models and their potential to contribute to future planning and the mitigation of landslide hazards in Kenya.*

**Key Words:** Landslide susceptibility, GIS, Kenya, weighted overlay, fuzzy logic

## 1. INTRODUCTION

Landslides pose significant threats worldwide, resulting in substantial economic losses, environmental damage, and societal impacts. With the expanding population and the encroachment of settlements into hazardous areas, the risks associated with landslides have intensified [1] [2] (Mugagga et al., 2012; Marshak, 2019). Geologists define landslides as the downslope movement of rocks or regolith (loose unconsolidated rock and soil) due to the force of gravity. These mass movements exhibit various characteristics, including composition, rate of movement, coherence, and the environment in which they occur, such as subaerial or submarine settings.

The occurrence of landslides is not limited to mountainous regions; they can happen in areas with low relief as well. Weather and climate patterns play a crucial role in landslide occurrence. Landslides are influenced by a combination of external triggering factors, such as over-steepened slopes, heavy rainfall, earthquakes, or volcanic eruptions, and internal inherent factors, including geological and morphological conditions. Geological factors comprise weak and weathered bedrock, jointed materials, fault lines, and variations in permeability. Human activities, such as improper land use, deforestation, excavation, and changes in groundwater systems, also contribute to landslides [2] [3] (Marshak, 2019; Varnes, 1978).

Kenya has experienced significant landslide incidents, primarily in the central highlands and southwestern regions (Figure 1). Heavy rainfall-induced landslides are common in the country [4] (Davies and Nyambok, 1993). The relationship between landslides and precipitation rates is evident, with notable events occurring during years with heavy rains. Anthropogenic factors, driven by population growth, have led to land degradation and an increase in landslide-prone areas [5] [6] (Larsson, 1989; Rob, 2011). Deforestation, particularly in districts bordering mountainous regions, exacerbates the problem [7] (Maina-Gichaba et al., 2013). While seismic and volcanic activities have not recently triggered landslides in Kenya, historical records indicate past occurrences associated with a 6.9 M earthquake in Subukia in 1928 [7] [8] (Maina-Gichaba et al., 2013; Mulwa et al., 2013).

The rise in landslide activities since the 1980s has resulted in severe social, economic, and environmental consequences, including loss of life, damage to agriculture, infrastructure, and property [9] [10] (Davies, 1996; Rowntree, 1989). Although available records indicate approximately 233 fatalities from landslides between 1986 and 2018, the actual number is likely much higher. Unfortunately, there is a lack of comprehensive data on the economic losses caused by landslides in Kenya, despite significant destruction to buildings, roads, railways, and waterways [11] (Ngecu and Mathu, 1999). The urgent need for reconstruction and assistance following landslides in western Kenya was estimated at \$18 million in 2013. Landslides also have detrimental environmental effects, with debris flows polluting rivers and impacting domestic livestock.

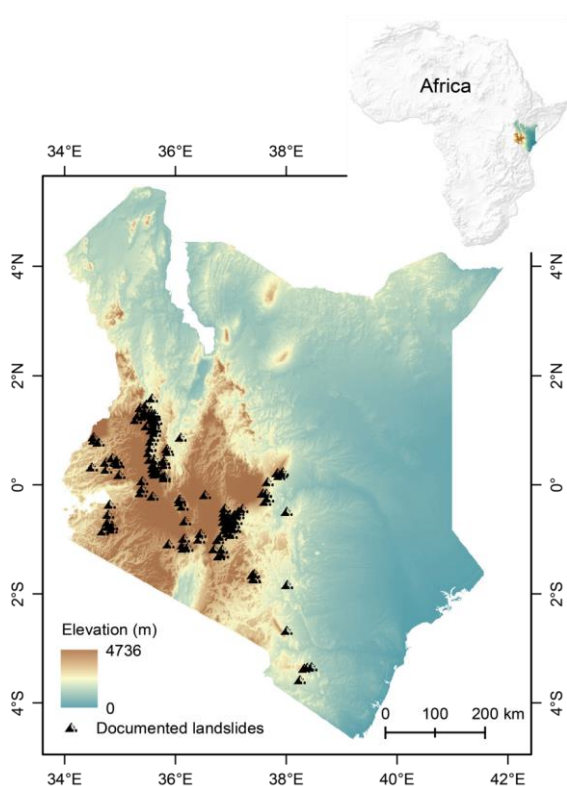


**Fig -1:** Location map of Kenya showing the documented landslides (black triangles). The hillshade is used as a base map.

To address these challenges, this study aims to assess landslide susceptibility in Kenya by integrating remote sensing and Geographic Information System (GIS) technologies. The specific objectives include (1) creating a landslide inventory map for the entire country, (2) acquiring and preparing necessary inputs for GIS modeling, (3) modeling landslide susceptibility, (4) validating outcomes through statistical analysis, and exploring the correlation between landslide cells and landslide events. By leveraging these tools and methods, a comprehensive understanding of landslide-prone areas can be achieved, aiding in effective hazard mitigation and informed decision-making for sustainable development in Kenya.

## 2. STUDY AREA AND PREVIOUS WORK

Situated in eastern Africa, the Republic of Kenya spans latitudes 5°30'N to 4°30'S and longitudes 34°00'E to 42°00'E (Figure 1). The country is divided by the equator into northern and southern regions, covering a land area of 581,61 km<sup>2</sup>. Kenya's equatorial location determines its climate, characterized by hot and humid conditions along the coast, temperate climates in the west and southwest, and hot and dry climates in the north and east [12] (Climates to Travel, 2019). The country experiences two rainy seasons: the long rains from March to May and the short rains from October to December. However, even between June and

September, the western highlands receive significant rainfall. Precipitation levels range from 800 to 2,000 mm annually in the southwestern part and coastal areas, while the arid zone receives less than 500 mm. Notably, the El Niño weather phenomenon, occurring between May 1997 and February 1998, brought prolonged heavy rainfall, resulting in numerous landslides across the country [11] (Ngecu and Mathu, 1999). Temperature variations range from 12°C to 36°C, with coastal regions experiencing average annual temperatures ranging from 22°C to 31°C and cooler temperatures of 12°C to 26°C in plateau areas. In 2018, Kenya's estimated population reached 51 million, representing a significant increase of 537% since 1960 when the population was 8 million [13] (The World Bank, 2019). The population is concentrated in high rainfall areas with fertile soil, and approximately 90% of the population resides in rural areas, relying on agriculture for their livelihoods [10] [14] (Rowntree, 1989; Ngecu and Ichang'i, 1999).

Kenya's topography can be classified into four major zones: the Coastal and Eastern Plains, the Central and Western Highlands, the Rift Valley Basin, and the Lake Victoria Basin. The Coastal and Eastern Plains cover approximately one-third of the country and have elevations ranging from sea level to 500 m. The Central and Western Highlands, separated by the Rift Valley Basin, encompass altitudes ranging from 1,500 to 5,200 m. The Rift Valley, a segment of the East African Rift System (EARS), runs predominantly in a north-south direction, with a maximum elevation of 500 m. The Lake Victoria Basin, including Lake Victoria itself, ranges in elevation from 500 to 1,000 m [14] (Ngecu and Mathu, 1999).

While numerous studies have explored landslides worldwide, limited research has focused specifically on landslides in Kenya [9] [14] [15] (Davies, 1996; Ngecu and Ichang'i, 1999; Kamau, 1981). Early investigations in the 1980s by Kamau (1981) and Rowntree (1989) examined mass movements in Kangema, Murang'a District, and conducted geographical assessments of landslides based on rational inference, respectively. Larsson (1986), Westerberg (1989), and Larsson (1989) studied landslides in the Central Kenya highlands, with the latter assessing the increase of landslides in relation to land-use changes on the slopes of Nyandarua [16] [17] [5]. Davies and Nyambok (1993) examined the Murang'a landslide that claimed eight lives on May 15, 1991, in Gacharage Village. Other studies explored landslides in Ol Kalou [18] (Johansson, 1993) and conducted multidisciplinary assessments encompassing geology, hydrology, landscape evaluation, agro-ecology, engineering, land use, and socioeconomics [19] (Christiansson et al., 1993). Ngecu and Ichang'i (1999) investigated a landslide event in Maringa village on April 30, 1997, along with its socioeconomic impact. Additionally, a few studies documented landslides triggered by the El Niño weather phenomenon during 1997-1998 [11] (Ngecu and Mathu, 1999). Subsequent studies explored landslide significance, distribution, and mitigation measures in Kenya and Uganda.

[20] (Nguru et al., 2004), rainfall-induced landslide probability in the central province [21] (Mwaniki et al., 2011), and the socioeconomic and environmental impacts of landslides in Kenya [7] (Maina-Gichaba et al., 2013). Remote sensing techniques were utilized to visualize and map past landslides in the central region of Kenya [22] [23] (Mwaniki et al., 2015a, 2015b), while GIS was employed to determine landslide potential in the western province [24] (Nyaberi, 2016). A study compared satellite image enhancement techniques for landslide identification and mapping in the central region using synthetic aperture radar and Landsat 8 imagery [25] (Mwaniki et al., 2017).

Existing studies have highlighted the socioeconomic impacts of landslides in Kenya and identified heavy rainfall in conjunction with natural geological and geomorphological conditions as primary causes of slope instability. Human activities, including road construction, excavation, and changes in land use, have also contributed to slope failures in the country. Despite these investigations, there is a lack of comprehensive publications assessing landslide hazards using GIS and remote sensing techniques for the entire country.

### 3. COMPILING THE DATASETS AND ESTABLISH THE LANDSLIDE INVENTORY

The accuracy and reliability of landslide modeling rely on the quantity and quality of data obtained through scientific methods and appropriate scaling [26] (Baeza and Corominas, 2001). However, in the case of Kenya, the availability and quality of geospatial data pose significant challenges. This research faced the daunting task of data acquisition and preparation, ensuring that only reliable and trustworthy data were utilized. Table 1 provides an overview of the raster and vector data obtained and created from various sources. Through meticulous data acquisition and preparation, this study ensures the utilization of reliable and comprehensive datasets to enhance the accuracy and effectiveness of landslide modeling in Kenya.

The vector boundary of Kenya was sourced from the World Resources Institute [27] (Ndeng'e et al., 2003). To construct a comprehensive landslide inventory for the entire country, landslide events from multiple sources were combined. Forty-six events were retrieved from the Open Data Portal - Global Landslide Catalog-NASA [28] (Kirschbaum et al., 2010), two events were obtained from Fatal Landslides [29] (Froude and Petley, 2018), and 82 events were derived from the landslide map of Kenya provided by the Mines and Geology Department (2012) [30]. Seismic records were downloaded from the United States Geological Survey (USGS) through the Earthquake Hazards Program [31]. Kenya experiences a low to moderate level of seismic activity, with most earthquakes ranging from 3.4 to 7 in magnitude and depths of 10 to 34 meters. Fault traces were obtained from the Global Faults layer accessible via ArcAtlas through Esri [32] (Finko, 2014). Stream and road data were

acquired from DIVA-GIS [33] (Hijmans et al., 2001). The soil map was extracted from the 2015 global soil map obtained from the United States Department of Agriculture–Natural Resources Conservation Service (USDA-NRCS) [34].

**Table -1:** Summary of the GIS datasets used in this study.

GIS layer	Type or resolution	Source
Administrative boundaries	Polygon	World Resources Institute
Landslide occurrences	Point	NASA & literature
Earthquakes	Point	USGS
Faults	Line	Esri
Drainages	Line	DIVA-GIS
Roads	Line	DIVA-GIS
Soil	Polygon	USDA-NRCS
Lithology	200 m	USGS
Land cover	30 m	RCMRD
Rainfall	800 m	World Resources Institute
DEM	30 m	USGS
Slope	30 m	This study

Raster data, including lithological units, were extracted from the World ELU 2015 geological map obtained from the USGS, which was developed through a collaborative partnership between the USGS and Esri [35] (Global Ecosystems). The main rock types encompass volcanic and metamorphic rocks, as well as unconsolidated sediments, with smaller extents of carbonate sedimentary rocks and evaporites. The land cover map of 2014 was generated through the Land Cover Change Mapping program in collaboration with the Department of Resource Surveys and Remote Sensing (DRSRS), the lead government organization, supported by the Regional Centre of Mapping of Resources for Development (RCMRD), Kenya Forest Service (KFS), and Survey of Kenya (SOK) (DRSRS, KFS, SOK & RCMRD, 2016) [36]. This map includes 11 different land cover types, such as grassland, cropland, vegetated wetland, forest, and others. Wooded and open grassland dominate the country's land cover. Precipitation records were obtained from the World Resources Institute [37] (Hijmans et al., 2005). The elevation map was derived from the 1 arc-sec Shuttle Radar Topographic Mission (SRTM) Digital Elevation Model (DEM) obtained from the USGS' EarthExplorer [38]. The slope map was generated from the 30-meter spatial resolution DEM, representing slope gradients ranging from 0% to 81%.

### 4. MODELING METHODOLOGY

The flowchart depicted in Figure 2 outlines the key steps and methodologies employed in this study, including the application of weighted overlay and fuzzy logic models. Due to the complex interactions among various causative factors, no single model can serve as the optimal solution for all landslide assessments. Empirical analysis methods, which examine past landslides to predict future occurrences under

similar triggering conditions, are suitable for local scales rather than global scales, as landslide causative factors vary by location [39] [40] [41] [42] (Guzzetti et al., 2008; Reichenbach et al., 1998; Sidle and Ochiai, 2006; Vennari et al., 2014). In this study, a multi-criteria decision-making method was employed to consider the relative contributions of each landslide causative factor, as it is well-suited and reliable for medium to regional scales [43] [44] [45] (Akgun, 2012; Ayalew and Yamagishi, 2005; Guzzetti et al., 1999).

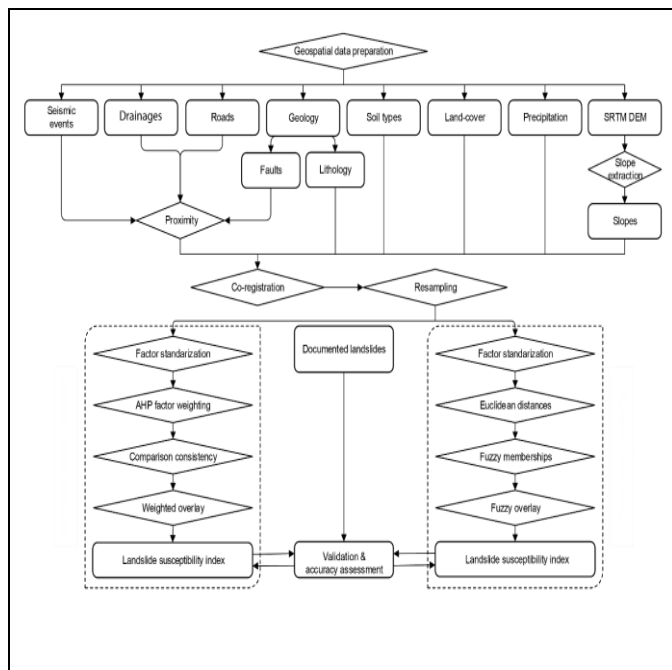


**Fig -2:** Flowchart showing the detailed steps of the modeling procedure.

#### 4.1 Determining and Reclassifying the Landslide Causative Factors

To identify which cells in each thematic factor layer have experienced landslides, a GIS tool for extracting multiple values was utilized. Through literature review and statistical analysis of the causative factors and the compiled landslide inventory map, ten factors were identified for landslide susceptibility assessment. As an example, the annual precipitation rate was chosen. The analysis revealed that only 1 landslide event (0.8%) occurred in areas with less than 600 mm/yr, 3 events (2.2%) in areas with precipitation rates between 600-700 mm/yr, 34 events (26.4%) in areas with rates between 700-1000 mm/yr, and 92 events (approximately 71% of the total) in areas with rates exceeding 1000 mm/yr. Based on this analysis, the latter class was considered the most susceptible to landslide occurrence. Accordingly, the precipitation rate layer was reclassified into four classes: <600, 600-700, 700-1000, and >1000 mm/yr, corresponding to low, medium, high, and very high susceptibility, respectively. Table 2 and Figures 3 and 4

display the documented landslides and their relationship with the assigned classes.

Factors that did not exhibit a discernible influence on landslide occurrence were excluded from further analysis. For instance, the distribution of landslides across the entire country with respect to aspect indicated that past landslides occurred on slopes with various orientations. Therefore, the slope aspect was not considered as a causative factor in this study.

To ensure consistency and compatibility, all thematic maps were clipped to the administrative boundaries of Kenya and projected into a common geographic coordinate system. The feature proximity (buffering) was applied, followed by the conversion of polygons to raster format and resampling to match the spatial resolution of the SRTM-DEM (30 m). Finally, the thematic maps were standardized into four linear classes and utilized in the weighted overlay model (Figure 3 and 4). Different classifications were considered for the fuzzy logic model, as explained in the fuzzy modeling section.

#### 4.2 Weighted Overlay Modeling

The weighted overlay model employed in this study incorporates the Analytic Hierarchy Process (AHP) for weighting the identified factors, followed by a weighted linear combination. AHP is a reliable method for assigning weights to multiple factors using a pairwise comparison matrix. It has been widely utilized in various fields to address real-world problems [46] [47] [48] [44] [49] (Guzzetti et al., 1999; Saaty, 1977, 1980; Saaty and Vargas, 1991; Ayalew and Yamagishi, 2005; Aly et al., 2005).

The pairwise comparison matrix involves comparing each factor with others based on its relative importance in relation to the problem at hand. Table 3 presents the scale ranging from 1 to 9, which is used for weighting the variables. The pairwise comparison matrix for the selected causative landslide factors is displayed in Table 4, where each cell represents the relative importance of the row factor in comparison to the corresponding column factor. Notably, the diagonal cells contain a value of 1 since they represent the comparison of each factor to itself. Solving the matrix and calculating the eigenvector yields weights that indicate the relative importance of each landslide factor.

To assess the matrix's consistency, the consistency ratio (CR) is computed, which reflects the likelihood that the ratings in the matrix were randomly assigned. The ratings are deemed acceptable when the consistency ratio is below 0.1. Consequently, the consistency index (CI) is calculated according to Equation 1, and CR is determined using

**Table -2:** Causative factors and corresponding classes with their relationship to the past landslides.

Causative factor	Corresponding class	# of landslides	Landslide (%)	Assigned class
Precipitation (mm/yr)	< 600	1	0.8	low
	600 – 700	3	2.2	medium
	700 – 1000	34	26.4	high
	>1000	92	70.6	very high
Lithology	Sedimentary rocks	0	0	low
	Unconsolidated	1	0.8	medium
	Metamorphic rocks	51	39.2	high
	Basaltic Volcanic rocks	78	60	very high
Elevation (m)	<800	0	0	low
	800-1200	15	11.5	medium
	1200-1700	34	26.2	high
	>1700	81	62.3	very high
Slope (%)	<2	7	5.4	low
	2-5	22	16.9	medium
	5-15	56	43.1	high
	>15	45	34.6	very high
Soil Type	Aridisols (1)	1	0.8	low
	Shifting sand (0)	0	0	low
	Alfisols (7)	7	5.4	medium
	Vetisols (1)	1	0.8	medium
	Entisola (10)	10	7.7	high
	Oxisols (18)	18	13.8	high
	Andisols (9)	9	6.9	high
	Inceptisols (39)	39	30	very high
	Ultisols (45)	45	34.6	very high
	Vegetated wetland	0	0	low
Land Cover	Open water	0	0	low
	Urban	3	2.3	medium
	Open forest	1	0.8	medium
	Moderate forest	4	3	medium
	Dense forest	16	12.3	high
	Open grassland	8	6.2	high
	Perennial cropland	8	6.2	high
	Wooded grassland	41	31.5	very high
	Annual cropland	49	37.7	very high
Fault Proximity (km)	>30	29	22.3	low
	20-30	11	8.5	medium
	10-20	34	26.2	high
	<10	56	43	very high
Earthquake Proximity (km)	>300	0	0	low
	200-300	0	0	medium
	100-200	32	24.6	high
	<100	98	75.4	very high
Drainages Proximity (m)	>300	120	92	low
	200-300	2	1	medium
	100-200	6	4	high
	<100	4	3	very high
Road Proximity (m)	>300	76	58.4%	low
	200-300	7	5.3%	medium
	100-200	18	14%	high
	<100	29	22.3%	very high

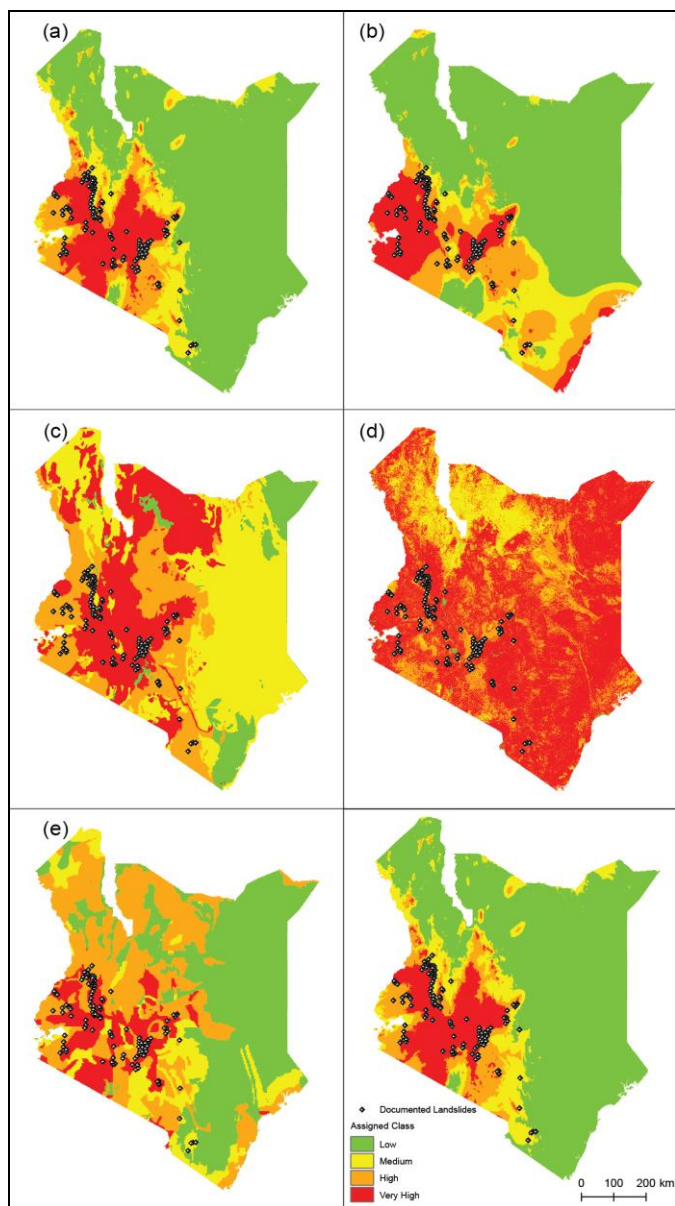


**Fig -3:** Factors used for the landslide susceptibility assessment, including elevation (a), precipitation (b), lithology (c), land cover (d), and soil (e).

Equation 2. In this study, a CR value of 0.0034 was achieved [46] [47] (Saaty, 1977, 1980).

$$CI = \frac{\lambda_{\max} - n}{n-1} \quad (1)$$

where  $\lambda_{\max}$  represents the principle of the largest eigenvalue in the matrix, and n indicates the number of landslide factors.

$$CR = \frac{CI}{RI} \quad (2)$$

where RI is the random index determined based on the matrix order as specified by Saaty (1977, 1980).

Factors that significantly contribute to landslide occurrence in Kenya, such as precipitation, lithology, and slope, were assigned the highest weights (as depicted in Table 4). Finally, a weighted linear combination was performed using the ten input data layers outlined in the flowchart to generate the landslide susceptibility index. In this process, each input raster layer is multiplied by its respective weight and then summed, resulting in the output value denoted by S in Equation 3 [50] (e.g., Eastman et al., 1995).

$$S = \sum W_i R_i \quad (3)$$

where S represents the landslide susceptibility, W denotes the weight of factor i, and R indicates the rank of factor i.

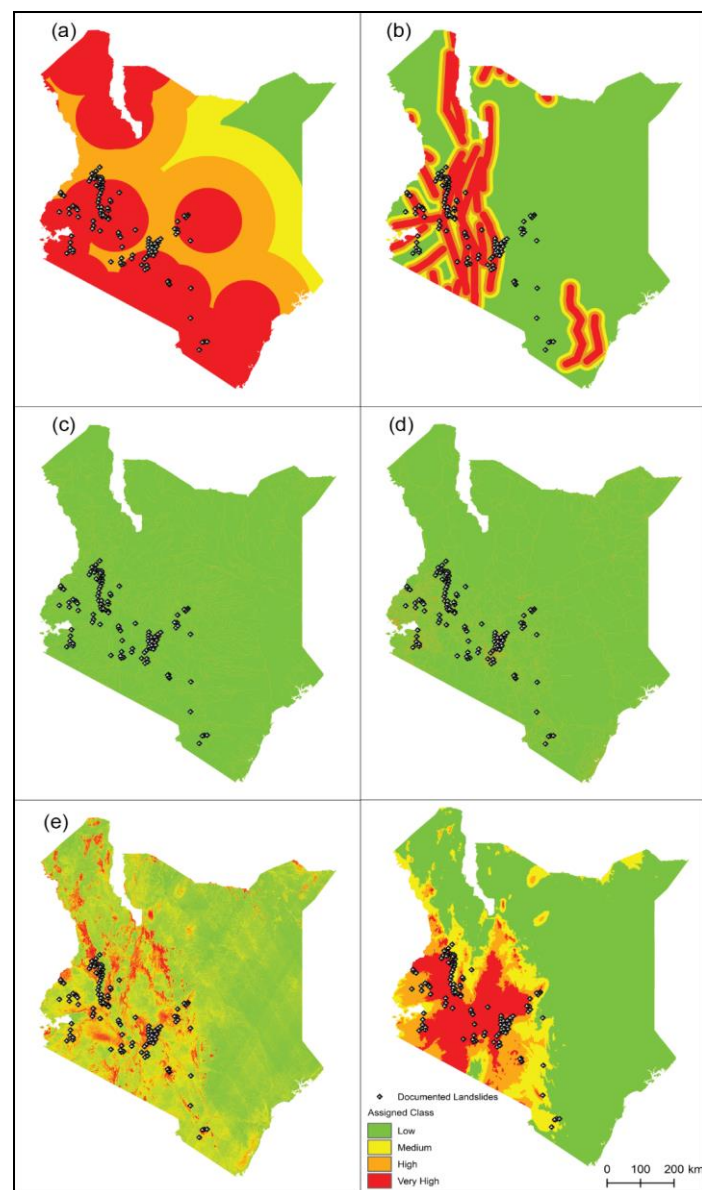


**Fig -4:** Factors used for the landslide susceptibility assessment, including earthquakes (a), faults (b), drainages (c), roads (d), and slope (e).

**Table -3:** Pairwise comparison scale (Saaty and Vargas 1991).

Scale	Definition
1	Equal importance
3	Moderate importance of one over another
5	Strong or essential importance
7	Very strong or demonstrated importance
9	Extreme importance
2, 4, 6, 8	Intermediate values
Reciprocals	For inverse comparison

#### 4.3 Fuzzy Logic Modeling

Fuzzy logic is a distribution-free approach designed to overcome the limitations of data-dependent approaches [51] (Kanungo et al., 2009). It was introduced by Zadeh (1965) as an alternative to the conventional Boolean set theory, which assigns objects binary values of 0 or 1. In contrast, fuzzy logic allows for the assignment of continuous values. A fuzzy set represents a class of objects with a continuum of membership ranks, characterized by a membership function that assigns values between 0 and 1 to each object. Fuzzy membership transforms input raster data into a layer with values ranging from 0 to 1, reflecting the probability of membership within a specific set. Fuzzy members within a set are assigned values  $> 0$  and  $\leq 1$ , while those outside the set are assigned 0. Various concepts can be applied to fuzzy sets, including inclusion, union, intersection, complement, relation, convexity, and other relationships, implemented using logical operators such as AND, OR, NOT, Product, Sum, and Gamma [52] [53] (Zadeh, 1965; Bonham-Carter, 1994).

In this study, fuzzy modeling was performed using algorithms implemented in ArcGIS, including Fuzzy Small, Fuzzy Near, and Fuzzy Linear. One of the key steps in fuzzy modeling and fuzzy memberships is the calculation of Euclidean distance, representing the shortest distance between two points. Euclidean distances were computed for four contributing variables: faults, earthquakes, drainages, and roads. Fuzzy Small was applied to faults, earthquakes, drainages, and roads, aiming for small input values for set membership with spread of 0.2, 2, 1, and 1, respectively. Figure 5 presents the results of applying Fuzzy Small to these variables with different values as shown in each figure. Fuzzy Near, on the other hand, assigns membership values near a specific value, with the midpoint assigned a membership of 1 and the end value assigned a membership of 0. For lithology, soil, and land cover raster factors, reclassification was performed to 6, 8, and 8 classes, respectively, with the highest value assigned a membership of 1. For example, in lithology, class 6 was assigned a membership of 1. Figure 6 provides an overview of this process. Linear data such as precipitation, slope, and elevation were transformed using the Fuzzy Linear transformation, as shown in Figure 7.

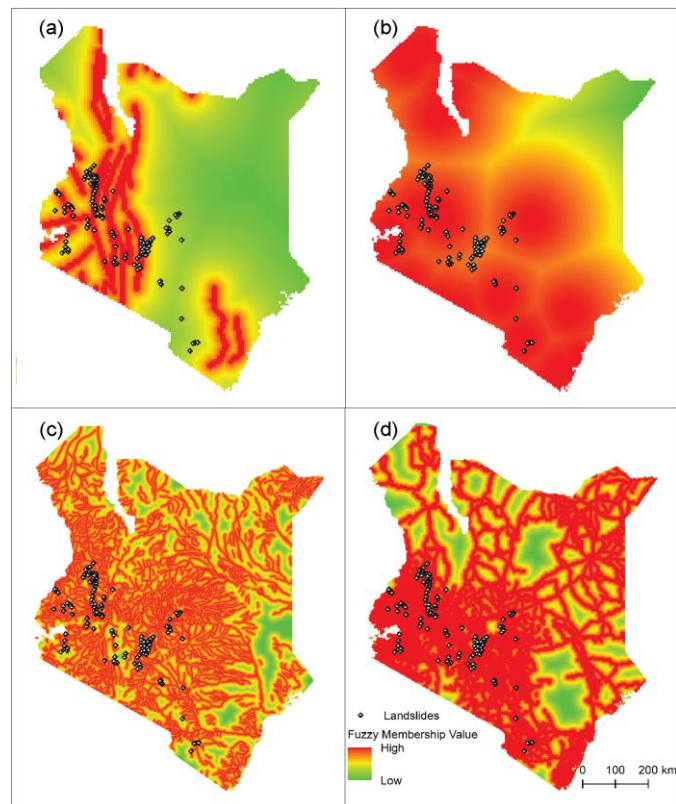


**Fig -5:** Fuzzy Small memberships including faults (a), earthquakes (b), drainages (c), and roads (d).

Ultimately, fuzzy overlay was applied to create the landslide susceptibility index using the Fuzzy Gamma operator, which has been effectively used in landslide susceptibility mapping [51] (e.g., Kanungo et al., 2009). The Fuzzy Gamma operator is expressed algebraically by Esri as a combination of Fuzzy Product and Sum, as shown in Equation 4:

$$\mu(x) = (\text{FuzzySum})^\gamma * (\text{FuzzyProduct})^{1-\gamma} \quad (4)$$

where  $\mu$  represents the fuzzy membership function,  $x$  represents the universe, and  $\gamma$  is a chosen value within the range of 0 to 1.

#### 4.4 Evaluating and Validation the Results

The evaluation of a landslide assessment model's quality is crucial to ensure its reliability and the production of acceptable results. The primary criterion for quality evaluation is the accuracy of the model, which involves examining the agreement between the modeled results and the observed data [54] (e.g., Frattini et al., 2010). In this study, the observed data consist of past documented landslide events represented in the landslide inventory, while the modeled results are the generated landslide susceptibility indices. Statistical analysis was conducted using Equation 5 to compare the known landslide occurrences with the produced landslide susceptibility

**Table -4:** Pairwise comparison matrix for the landslide susceptibility index.

Factor	Precipitation	Lithology	Slope	Elevation	Soil	Land cover	Faults	Earthquakes	Drainages	Roads	Weight
Precipitation	1.00	3.00	3.00	5.00	6.00	6.00	7.00	7.00	8.00	9.00	0.30
Lithology	0.33	1.00	1.00	4.00	5.00	5.00	6.00	6.00	7.00	8.00	0.19
Slope	0.33	1.00	1.00	4.00	5.00	5.00	6.00	6.00	7.00	8.00	0.19
Elevation	0.20	0.25	0.25	1.00	4.00	4.00	5.00	5.00	6.00	7.00	0.11
Soil	0.17	0.20	0.20	0.25	1.00	1.00	4.00	4.00	5.00	6.00	0.06
Land cover	0.17	0.20	0.20	0.25	1.00	1.00	4.00	4.00	5.00	6.00	0.06
Faults	0.14	0.17	0.17	0.20	0.25	0.25	1.00	1.00	4.00	5.00	0.03
Earthquakes	0.14	0.17	0.17	0.20	0.25	0.25	1.00	1.00	4.00	5.00	0.03
Drainages	0.13	0.14	0.14	0.17	0.20	0.20	0.25	0.25	1.00	2.00	0.02
Roads	0.11	0.13	0.13	0.14	0.17	0.17	0.20	0.20	0.33	1.00	0.01
CI = 0.0051											
RI = 1.49											
CR = 0.0034											

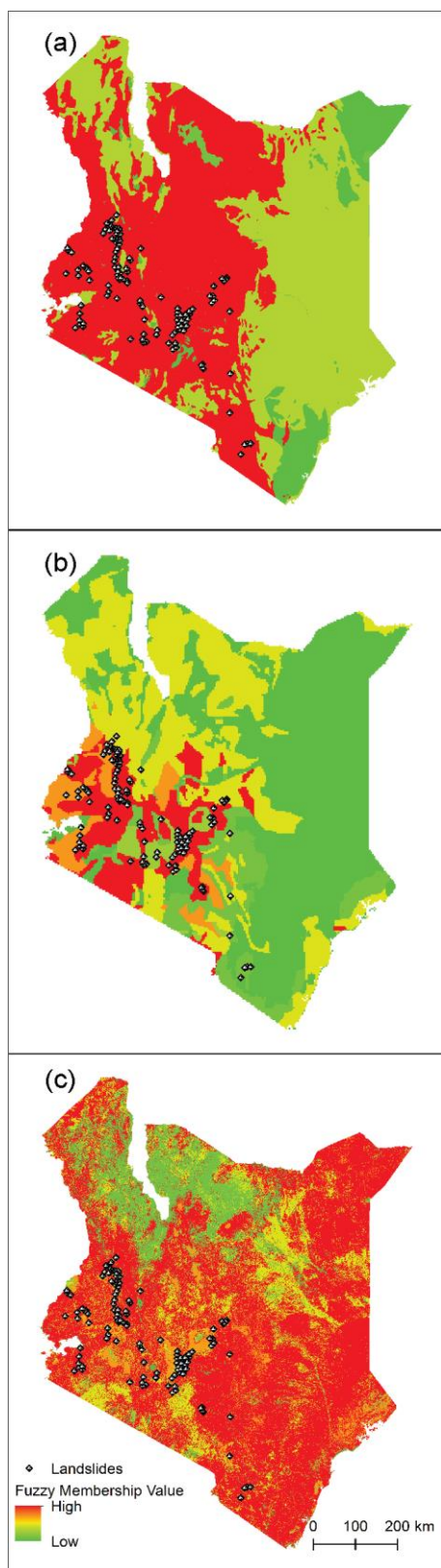


**Fig -6:** Fuzzy Near memberships including lithology (a), soil (b), and land cover (c).

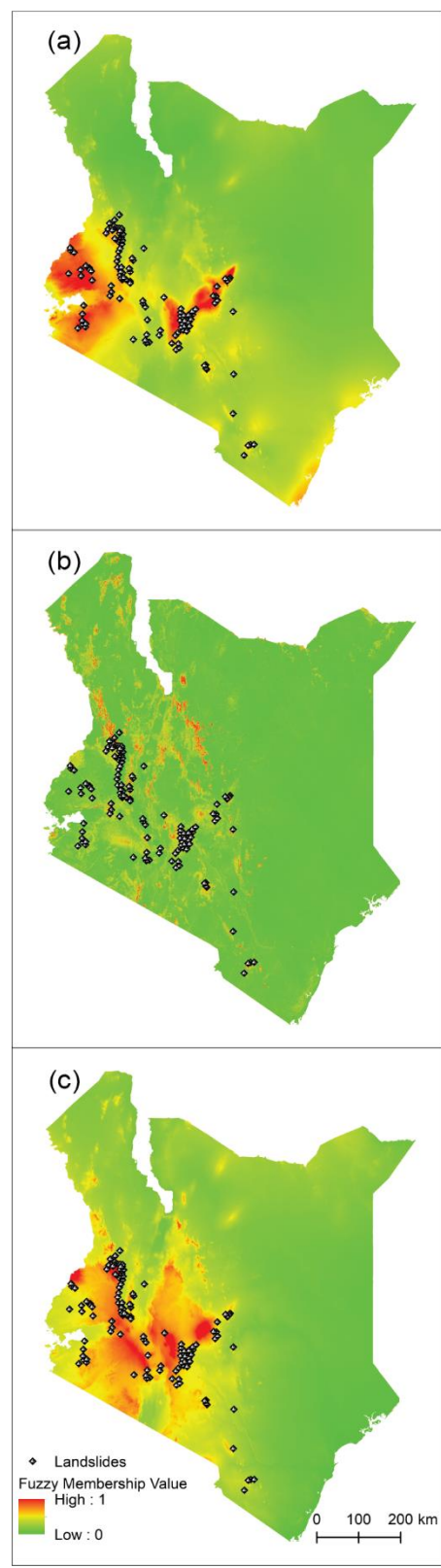


**Fig -7:** Fuzzy Linear memberships including precipitation (a), slope (b), and elevation (c).

indices. This analysis provides a quantitative measure of how well the model aligns with the observed landslide occurrences, allowing for an assessment of the model's performance and reliability.

$$A = (N/T)100 \quad (5)$$

where A represents the average model accuracy, N denotes the number of landslides within each susceptibility index, and T is the total number of landslides.

## 5. RESULTS AND DISCUSSIONS

This study has produced valuable outcomes in the form of a landslide inventory map and two landslide susceptibility models. The landslide inventory map displays the distribution of past and current landslides in Kenya, encompassing 130 events that occurred between 1928 and 2018 (Figure 1). It is important to note that the accuracy of the susceptibility models relies on the available documented landslide data, and further improvements could be achieved with a larger number of recorded events. Nonetheless, the created models remain reliable and offer utility for future planning and mitigating landslide hazards in Kenya.

The central and southwestern regions of Kenya exhibit the highest susceptibility to landslides, as indicated by the two susceptibility models. These areas are characterized by a combination of factors including high rainfall, steep slopes, and weathered soil and bedrock conditions. The weighted overlay model classifies Kenya into four susceptibility index classes (Figure 8.a): low, medium, high, and very high, covering approximately 34%, 40%, 22%, and 4% of the total area, respectively (Table 5). The high and very high susceptibility classes encompass about 26% of the entire country, corresponding to an area of 151,22 km<sup>2</sup> that is vulnerable to active landslides.

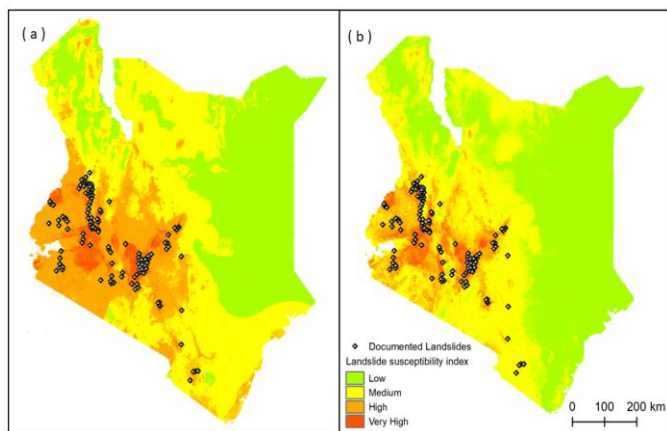


**Fig -8:** Landslide index created by the weighted overlay (a). Landslide susceptibility index created by the fuzzy logic (b).

**Table -5:** Statistical analysis for the landslide index created by the weighted overlay (WO) and fuzzy logic (FZ) with the accuracy correlation for the two models (values are in %).

Hazard Index	Index %		# of past landslides		Fuzzy Index Value	Accuracy correlation %	
	WO	FZ	WO	FZ		WO	FUZZY
Low	34	68	0	0	< 0.3	0	0
Medium	40	19	4	20	0.3 – 0.5	3	15.4
High	22	10	56	46	0.5 – 0.6	43	35.4
Very high	4	3	70	64	> 0.6	54	49.2

In contrast, the fuzzy logic model produces a distinct output for landslide susceptibility, with pixel values ranging from 0 to 0.85. It also categorizes the country into four main classes (Figure 8.b): low, medium, high, and very high, representing approximately 68%, 19%, 10%, and 3% of Kenya's area, respectively (Table 5). These percentages differ from those calculated by the weighted overlay model due to the variations in factor standardization approaches employed in each modeling procedure. Statistical analysis reveals that the weighted overlay model reports no landslide events in the low index, only 4 events in the medium index, and 126 events in the high and very high indices (Table 5). Conversely, the fuzzy model has no landslides reported in the low index, 20 in the medium index, and 110 in the high and very high indices (Table 5). When considering the high and very high indices of both models, the weighted overlay model achieves an accuracy of 97%, compared to 85% for the fuzzy logic model (Table 5).

Unfortunately, the areas most prone to landslides are also the most agriculturally productive and densely populated in Kenya, owing to their high precipitation rates and fertile soils. Long-term land use changes may have contributed to increased landslide occurrences in these areas. To mitigate landslide hazards in such regions, it is crucial to avoid construction on steep slopes and existing landslides. Cultivation, deforestation, and settlement should be minimized in steep slope areas. However, if building on gentle slopes becomes necessary, slope stabilization measures should be considered. Planting deep-rooted trees on steep slopes can also help mitigate landslides. Additionally, geodetic monitoring should be implemented in areas prone to active landslides. There is a pressing need for the development of a comprehensive landslide management program in Kenya to assess landslide hazards and associated risks effectively.

## 6. CONCLUSIONS

Landslides are a prevalent phenomenon in the mountainous regions of Kenya, emphasizing the importance of landslide hazard assessment, particularly in the central and

southwestern parts of the country. This study successfully created a landslide inventory map, encompassing 130 past landslide events, by compiling records from various reliable sources. Subsequently, two models, the weighted overlay model and the fuzzy logic model, were employed to compute landslide susceptibility indices.

The accuracy of the models heavily relies on the limited number of documented landslide events and the identified causative and triggering factors. The weighted overlay model exhibited a high accuracy, with approximately 97% of the past landslides occurring in the high and very high susceptibility indices, compared to 85% for the fuzzy logic model. These variations can be attributed to the different approaches employed for factor categorization and standardization in each model.

The results from the weighted overlay model indicate that approximately 26% of Kenya's land area is susceptible to landslides. As the first comprehensive landslide study conducted for the entire country, this research significantly enhances our understanding of landslide hazards and provides valuable insights for decision-makers in future planning and mitigating associated risks in Kenya.

Furthermore, this study underscores the effectiveness of geospatial technologies in landslide assessments and emphasizes the need for ongoing geodetic monitoring in the central and southwestern regions of Kenya, which are particularly vulnerable to active landslides. By predicting potential disastrous events, geodetic monitoring can play a vital role in safeguarding lives and infrastructure. This study contributes to the advancement of landslide research in Kenya and highlights the importance of proactive measures to address landslide hazards. Continued efforts in landslide monitoring, research, and implementation of appropriate mitigation strategies are crucial for the sustainable development and safety of communities in landslide-prone areas of Kenya.

## ACKNOWLEDGEMENT

Thanks to InSAR Research Group at the University of Arkansas for the discussions and valuable comments. Thanks also to the World Resources Institute, NASA: National Aeronautics and Space Administration, USGS: United States Geological Survey, Esri: Environmental Systems Research Institute, USDA-NRCS: the United States Department of Agriculture–Natural Resources Conservation Service, RCMRD: Regional Centre for Mapping of Resources for Development, and DIVA-GIs for providing the necessary data for this research.

## REFERENCES

- [1] Mugagga, F., Kakembo, V., & Buyinza, M. 2012. "Land use changes on the slopes of Mount Elgon and the implications for the occurrence of landslides." *CATENA*, 90, 39–46. <https://doi.org/10.1016/j.catena.2011.11.004>.
- [2] Marshak S. 2019. *Essentials of geology* (Sixth edition). New York: W.W. Norton & Company.
- [3] Varnes DJ. 1978. Slope movement types and processes. In *Landslides—Analysis and control*: National Research Council, Washington, D.C., Transportation Research Board; p. 234. The University of California: National Academy of Sciences.
- [4] Davies TC, Nyambok IO. 1993. "The Murang'a landslide, Kenya." *Environmental Geology* 21(1–2):19–21. <https://doi.org/10.1007/BF00775046>.
- [5] Larsson M. 1989. "Landslides in the mountain areas of Kenya: comparative studies of different slopes within the Nyandarua Range." In: *Soil and Water Conservation in Kenya* (Edited by Thomas DB, Biamah EK, Kilewe AM, Lundgren L, Mochoge BO) pp123-136. Proceedings Third National Workshop, Kabete, Nairobi.
- [6] Rob BK. 2011. "Landslide disaster vulnerability in Western Kenya and mitigation options: A synopsis of evidence and issues of Kuvasali landslide." *Journal of Environmental Science and Engineering* 5(1):110–115.
- [7] Maina-Gichaba C, Kipseba EK, Masibo M. 2013. "Overview of landslide occurrences in Kenya." In *Developments in Earth Surface Processes*. 16:293–314. <https://doi.org/10.1016/B978-0-444-59559-1.00020-7>.
- [8] Mulwa JK, Kimata F, Duong NA. 2013. "Seismic hazard." In *Developments in Earth Surface Processes*. 16:267–292. <https://doi.org/10.1016/B978-0-444-59559-1.00019-0>.
- [9] Davies TC. 1996. "Landslide research in Kenya." *Journal of African Earth Sciences* 23(4):541–545. [https://doi.org/10.1016/S0899-5362\(97\)00017-1](https://doi.org/10.1016/S0899-5362(97)00017-1).
- [10] Rowntree KM. 1989. *Landslides in Kenya: A geographical appraisal*. In: Brabb EE and Harrod BL (Eds), *Landslides: Extent and economic significance*; p. 253–259. Rotterdam: A.A. Balkema.
- [11] Ngecu WM, Mathu EM. 1999. "The El Niño-triggered landslides and their socioeconomic impact on Kenya." *Environmental Geology* 38(4):277–284. <https://doi.org/10.1007/s002540050425>.
- [12] Climates to Travel. 2019. Climate - Kenya. [accessed 2019 Feb 22]. <https://www.climatestotravel.com/climate/kenya>.
- [13] The World Bank. 2019. Data, Kenya. [accessed 2019 Feb 27]. <https://data.worldbank.org/country/kenya>.
- [14] Ngecu WM, Ichang'i DW. 1999. "The environmental impact of landslides on the population living on the eastern footslopes of the Aberdare ranges in Kenya: A case study of Maringa Village landslide." *Environmental*

- Geology 38(3):259–264.  
<https://doi.org/10.1007/s002540050423>.
- [15] Kamau NI. 1981. A study of mass movements in Kangema area, Murang'a District, Kenya [Project report, postgraduate diploma in soil conservation]. University of Nairobi.
- [16] Larsson M. 1986. Landslides in the mountain dress of Kenya: causes, effects and rehabilitation. Unpubl. research proposal, 93p. Department of Physical Geography, Stockholm University.
- [17] Westerberg LO. 1989. "Rainfall characteristics, soil properties, land-use and landslide erosion in the Kanyenyaini area, Nyandarua Range, Kenya." M. Sc. thesis., Department of Physical Geography, Stockholm University.
- [18] Johansson A. 1993. A study of earth flow features and the relation to soil and rainfall characteristics in Ol'Joro Orok Division, Nyandarua District, Kenya. Unpubl. B. Sc. degree project report. Department of Physical Geography. Stockholm University.
- [19] Christiansson C, Zobisch M, Lunden B, Davies TC, Westerberg LO, Mburu D, Granit J. 1993. Landslides and related processes in Murang'a District, Central Kenya highlands. A proposal, EDSU, University of Stockholm/DAE, University of Nairobi; 10p.
- [20] Ngecu WM, Nyamai CM, Erima G. 2004. "The extent and significance of mass-movements in Eastern Africa: Case studies of some major landslides in Uganda and Kenya." Environmental Geology 46(8):1123–1133. <https://doi.org/10.1007/s00254-004-1116-y>.
- [21] Mwaniki MW, Ngigi T, Waithaka E. 2011. Rainfall induced landslide probability mapping for Central Province. <https://doi.org/10.13140/rg.2.1.4509.9046>.
- [22] Mwaniki MW, Möller M, Schellmann G. 2015a. Landslide inventory using knowledge based multi-sources classification time series mapping: A case study of central region of Kenya. GI\_Forum.1:209–219. <https://doi.org/10.1553/giscience2015s209>.
- [23] Mwaniki MW, Agutu NO, Mbaka JG, Ngigi TG, Waithaka EH. 2015b. "Landslide scar/soil erodibility mapping using Landsat TM/ETM+ bands 7 and 3 Normalised Difference Index: A case study of central region of Kenya." Applied Geography 64:108–120. <https://doi.org/10.1016/j.apgeog.2015.09.009>.
- [24] Nyaberi GN. 2016. Analysing landslide potentiality of former Western Province Kenya using GIS. Unpublished paper.
- [25] Mwaniki MW, Kuria DN, Boitt MK, Ngigi TG. 2017. "Image enhancements of Landsat 8 (OLI) and SAR data for preliminary landslide identification and mapping applied to the central region of Kenya." Geomorphology 282:162–175. <https://doi.org/10.1016/j.geomorph.2017.01.015>.
- [26] Baeza C, Corominas J. 2001. "Assessment of shallow landslide susceptibility by means of multivariate statistical techniques." Earth Surface Processes and Landforms 26(12):1251–1263. <https://doi.org/10.1002/esp.263>.
- [27] Ndeng'e G, Opiyo C, Mistiaen J, Krstjanson P. 2003. "Geographic dimensions of well-being in Kenya, where are the poor? From districts to locations (volume one). Kenya. Ministry of Planning and National Development. Nairobi, Kenya: Central Bureau of Statistics." Retrieved from <http://datasets.wri.org/dataset/district-administrative-boundaries-of-kenya>.
- [28] Kirschbaum DB, Adler R, Hong Y, Hill S, Lerner-Lam A. 2010. "A global landslide catalog for hazard applications: Method, results, and limitations." Natural Hazards 52(3):561–575. <https://doi.org/10.1007/s11069-009-9401-4>.
- [29] Froude MJ, Petley DN. 2018. "Global fatal landslide occurrence from 2004 to 2016." Natural Hazards and Earth System Sciences 18(8):2161–2181. <https://doi.org/10.5194/nhess-18-2161-2018>.
- [30] Mines and Geology Department. 2012. Map of landslide in Kenya [Unpublished].
- [31] USGS. Earthquake Hazards Program. [accessed 2019 Jan 10]. <https://earthquake.usgs.gov/earthquakes/map/>.
- [32] Finko EA. 2014. Global faults layer from ArcAtlas (Esri). [accessed 2019 Jan 22]. <https://www.arcgis.com/home/item.html?id=a5496011fa494b99810e4deb5c618ae2>.
- [33] Hijmans RJ, Guarino L, Cruz M, Rojas E. 2001. "Computer tools for spatial analysis of plant genetic resources data: 1. DIVA-GIS." Plant Genet Resources Newsletter 127:15–19.
- [34] USDA-NRCS. [accessed 2019 Jan 12]. <https://www.nrcs.usda.gov/wps/portal/nrcs/site/national/home/>.
- [35] Global Ecosystems. 2019. [accessed 2019 Jan 15]. <https://rmgsc.cr.usgs.gov/ecosystems/datadownload.shtml>.
- [36] DRERS, KFS, SOK, RCMRD. 2016. "Land cover change mapping to support the system for land-based emissions estimation in Kenya (SLEEK)." Retrieved from Regional Centre for Mapping of Resources for Development website: <https://www.rcmrd.org/sleek>.
- [37] Hijmans RJ, Cameron S, Parra J. 2005. WorldClim climate surfaces, version 1.4. [accessed 2019 Jan 10]. <http://www.worldclim.org/>.

- [38] EarthExplorer. 2019. [accessed 2019 Jan 20]. <https://earthexplorer.usgs.gov/>.
- [39] Guzzetti F, Peruccacci S, Rossi M, Stark CP. 2008. "The rainfall intensity-duration control of shallow landslides and debris flows: An update." *Landslides* 5(1):3–17. <https://doi.org/10.1007/s10346-007-0112-1>.
- [40] Reichenbach P, Cardinali M, De Vita P, Guzzetti F. 1998. "Regional hydrological thresholds for landslides and floods in the Tiber River Basin (central Italy)." *Environmental Geology* 35(2–3):146–159. <https://doi.org/10.1007/s002540050301>.
- [41] Sidle RC, Ochiai H. 2006. Landslides: Processes, prediction, and land use. <https://doi.org/10.1029/WM018>.
- [42] Vennari C, Gariano SL, Antronico L, Brunetti MT, Iovine G, Peruccacci S, Guzzetti F. 2014. "Rainfall thresholds for shallow landslide occurrence in Calabria, southern Italy." *Natural Hazards and Earth System Sciences* 14(2):317–330. <https://doi.org/10.5194/nhess-14-317-2014>.
- [43] Akgun A. 2012. "A comparison of landslide susceptibility maps produced by logistic regression, multi-criteria decision, and likelihood ratio methods: A case study at Izmir, Turkey." *Landslides* 9(1):93–106. <https://doi.org/10.1007/s10346-011-0283-7>.
- [44] Ayalew L, Yamagishi H. 2005. "The application of GIS-based logistic regression for landslide susceptibility mapping in the Kakuda-Yahiko Mountains, Central Japan." *Geomorphology* 65(1–2):15–31. <https://doi.org/10.1016/j.geomorph.2004.06.010>.
- [45] Guzzetti F, Carrara A, Cardinali M, Reichenbach P. 1999. "Landslide hazard evaluation: A review of current techniques and their application in a multi-scale study, Central Italy." *Geomorphology* 31(1–4):181–216. [https://doi.org/10.1016/S0169-555X\(99\)00078-1](https://doi.org/10.1016/S0169-555X(99)00078-1).
- [46] Saaty TL. 1977. "A scaling method for priorities in hierarchical structures." *Journal of Mathematical Psychology* 15(3):234–281. [https://doi.org/10.1016/0022-2496\(77\)90033-5](https://doi.org/10.1016/0022-2496(77)90033-5).
- [47] Saaty TL. 1980. *The analytic hierarchy process: Planning, priority setting, resource allocation*. New York; London: McGraw-Hill International Book Co.
- [48] Saaty TL, Vargas LG. 1991. *Prediction, projection, and forecasting: Applications of the analytic hierarchy process in economics, finance, politics, games, and sports*. Boston: Kluwer Academic Publishers.
- [49] Aly MH, Giardino JR, Klein AG. 2005. Suitability assessment for New Minia City Egypt: A GIS approach to engineering geology. *Environmental and Engineering Geoscience* 11(3):259–269. <https://doi.org/10.2113/11.3.259>.
- [50] Eastman JR, Jin W, Kyem P, Toledano J. 1995. "Raster procedure for multi-criteria/multi-objective decisions." *Photogrammetric Engineering and Remote Sensing* 61(5):539–547.
- [51] Kanungo DP, Arora MK, Sarkar S, Gupta RP. 2009. "Landslide susceptibility zonation (LSZ) Mapping." *Journal of South Asia Disaster Studies* 2(1):81–105.
- [52] Zadeh LA. 1965. "Fuzzy sets." *Information and Control* 8(3):338–353. [https://doi.org/10.1016/S0019-9958\(65\)90241-X](https://doi.org/10.1016/S0019-9958(65)90241-X).
- [53] Bonham-Carter G. 1994. *Geographic information systems for geoscientists: Modelling with GIS* (1st ed). Oxford; New York: Pergamon.
- [54] Frattini P, Crosta G, Carrara A. 2010. "Techniques for evaluating the performance of landslide susceptibility models." *Engineering Geology* 111(1–4):62–72. <https://doi.org/10.1016/j.enggeo.2009.12.004>.